BIOCHEMISTRY
including biophysical chemistry & molecular biology

Article

pubs.acs.org/biochemistry

Substrate Recognition and Specificity of Double-Stranded RNA Binding Proteins

Lela Vuković,*[,†,‡] Hye Ran Koh,[†,‡] Sua Myong,*[,‡,§] and Klaus Schulten*[,†,‡]

[†]Department of Physics, University of Illinois at Urbana—Champaign, Urbana, Illinois 61801, United States

[‡]Center for the Physics of Living Cells, University of Illinois at Urbana—Champaign, Urbana, Illinois 61801, United States

[§]Department of Bioengineering, University of Illinois at Urbana—Champaign, Urbana, Illinois 61801, United States

Supporting Information

ABSTRACT: Recognition of double-stranded (ds) RNA is an important part of many cellular pathways, including RNA silencing, viral recognition, RNA editing, processing, and transport. dsRNA recognition is often achieved by dsRNA binding domains (dsRBDs). We use atomistic molecular dynamics simulations to examine the binding interface of the transactivation response RNA binding protein (TRBP) dsRBDs to dsRNA substrates. Our results explain the exclusive selectivity of dsRBDs toward dsRNA and against DNA−RNA hybrid and dsDNA duplexes. We also provide corresponding experimental evidence. The dsRNA duplex is recognized by dsRBDs through the A-form of three duplex grooves and by the chemical properties of RNA bases, which have 2′-hydroxyl groups on their sugar rings. Our simulations show that TRBP dsRBD discriminates dsRNA- from DNA-containing duplexes primarily through interactions at two duplex grooves. The simulations also reveal that the conformation of the DNA−RNA duplex can be altered by dsRBD proteins, resulting in a weak binding of dsRBDs to DNA−RNA hybrids. Our study reveals the structural and molecular basis of protein−RNA interaction that gives rise to the observed substrate specificity of dsRNA binding proteins.

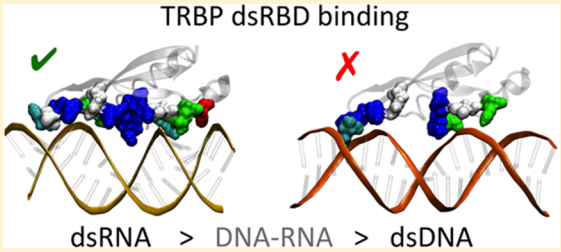

1. INTRODUCTION

RNA is emerging as an important regulatory element of many cellular processes.[1−4] Double stranded (ds) RNA is a frequent structural element of the cellular RNA; accordingly, cells synthesize many proteins that recognize it. dsRNA binding domain (dsRBD) is one of the most abundant RNA binding domains,[5,6] found in proteins localized in both cell nuclei and cytoplasm.[7] dsRBD proteins primarily regulate gene expression and signaling events. For example, the protein kinase PKR binds viral dsRNA and signals the onset of infection;[8] RNA helicase A (RHA) unwinds dsRNA;[9] the Dicer enzyme binds to and slices dsRNA into 21−22 nucleotide long pieces, which silence mRNA;[10,11] adenosine deaminase acting on RNA (ADAR) edits adenosine bases of dsRNA and converts them to inosines.[12] Many dsRBD proteins contain multiple dsRBDs. For example, two dsRBDs are found in RHA, three dsRBDs are found in ADAR1, in protein activator of PKR (PACT), and in transactivation response RNA binding protein (TRBP), and five dsRBDs are found in Staufen.[7]

TRBP participates in multiple cellular pathways in cell nuclei and cytoplasm.[13] In gene silencing by the RNA interference pathway, TRBP, Dicer, and PACT proteins are essential components of the RNA-induced silencing complex.[14−17] Biochemical and cryo-electron microscopy experiments have shown that two of TRBP dsRBDs aid in positioning of dsRNA in the proper conformation for dsRNA cutting by Dicer.[18] Recent single molecule experiments established that TRBP and Dicer-TRBP bind to and diffuse on dsRNA duplexes.[19] Interestingly, TRBP does not bind to duplex types other than dsRNA, namely not to dsDNA and not to DNA−RNA hybrids.[19,20] Many other dsRBD proteins specifically bind to dsRNA duplexes, whereas some also weakly bind to DNA−RNA hybrid duplexes.[21,22]

Considering the above experimental data about dsRBD binding targets, there are two questions of particular interest: (1) How do dsRBDs discriminate between nucleic acid duplexes of similar structures, such as dsRNA, DNA−RNA, and dsDNA? (2) How do dsRBDs discriminate between dsRNA of different sequences, abundant in the cell nuclei and cytoplasm? In the present study, we address the first question. Currently, the mechanism of dsRBD discrimination of dsRNA, DNA−RNA, and dsDNA has been explored only through static (crystal) structures of several different dsRBDs to short pieces of dsRNA[5] and short (2 ns) simulations.[23] Here, we examine by experiments and atomistic molecular dynamics (MD) simulations the binding of TRBP dsRBDs to dsRNA, DNA−RNA, and dsDNA duplexes. Our simulations identify the molecular mechanism of dsRNA recognition by dsRBDs; in particular, they reveal why dsRBDs bind weakly to DNA−RNA duplexes but do not bind to dsDNA duplexes.

Received: March 22, 2014
Revised: May 1, 2014
Published: May 6, 2014

 © 2014 American Chemical Society

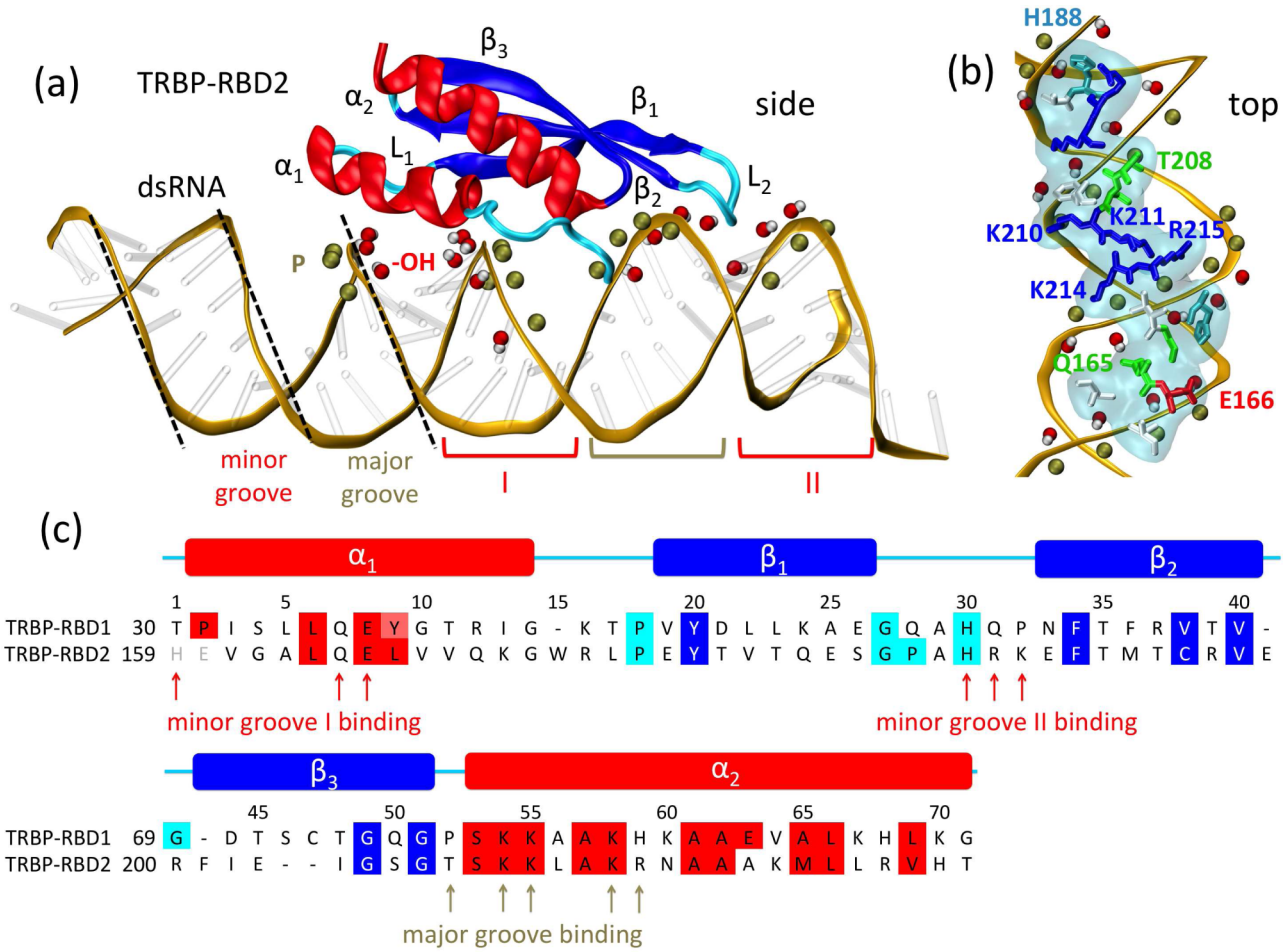

Figure 1. Binding of TRBP-RBD2 to dsRNA. (a) Snapshot of the TRBP-RBD2:dsRNA complex. TRBP-RBD2 binds to dsRNA across three grooves, in minor−major−minor groove pattern. dsRNA minor grooves are lined with 2′ hydroxyl groups (for clarity, only shown at the binding interface as red and white spheres), and its major grooves are lined with phosphate groups (P atoms are shown as tan spheres). Minor and major grooves, which interact with TRBP-RBD2, are marked with red and tan brackets, respectively, the two minor grooves being distinguished by labels I and II. The RNA backbone is shown in gold, the bases are shown as transparent sticks, and TRBP-RBD2 is colored according to its secondary structure, where helices are shown in red, β-sheets in blue, and unstructured loops in cyan. (b) Top view of the binding interface of the TRBP-RBD2:dsRNA complex. TRBP-RBD2 residues within 3 Å of the dsRNA are shown both as a transparent surface and in licorice representation. Blue residues are positively charged, red residues are negatively charged, green and cyan residues are polar, and white residues are nonpolar. (c) Sequence alignment of two TRBP dsRBDs. The residues conserved across different species and proteins are highlighted (Figure S1 (Supporting Information) and ref 5), where the colors indicate secondary structure elements, as shown in (a). The arrows point to TRBP-RBD2 residues that contact dsRNA; red and tan arrows mark minor and major groove contacts, respectively.

2. METHODS

Electrophoretic Mobility Shift Assay. To experimentally investigate binding of TRBP-RBD2 to dsRNA, DNA−RNA, and dsDNA, we performed an electrophoretic mobility shift assay (EMSA). We prepared three types of 25-bp duplexes with the same sequence (*forward*, 5′-GCUUGUCGGGAGCGC-CACCCUCUGC-3′; *reverse*, 5′-GCAGAGGGUGGCG-CUCCCGACAAGC-3′; T instead of U for DNA strands), which were labeled with either DY547 or Cy3 at the 3′ end of the reverse strand. We incubated 10 nM of 25-bp duplexes with various concentrations of TRBP-RBD2 ranging from 1 to 10 μM in binding buffer (20 mM Tris−HCl, pH 7.5, 25 mM NaCl, 1 mM DTT, and 0.1 mg/mL BSA) on the ice for 20 min. Then, 8 μL of the incubated sample was mixed with 2 μL of RNA loading dye (NEB) and the mixture was loaded immediately in the 6% DNA retardation gel (Invitrogen). We took the fluorescence gel images after running the gel at 100 V for 40 min and analyzed the band density with ImageJ (http://rsbweb.nih.gov/ij/).

Atomic Resolution Models. To examine mechanisms of dsRNA recognition by dsRBD domains, we simulated three complexes: (i) TRBP-RBD2:dsRNA, (ii) TRBP-RBD2:DNA−RNA, and (iii) TRBP-RBD2:dsDNA, where TRBP-RBD2 labels the second dsRBD of TRBP. The TRBP-RBD1:dsRNA complex and dsRNA, DNA−RNA, and dsDNA duplexes were simulated also separately for comparison. The initial structures of complexes i−iii were based on the crystal structure of TRBP-RBD2 bound to coaxially stacked RNA duplexes (Protein Data Bank entry code 3ADL).[24] The initial structures of dsRNA, DNA, and DNA−RNA duplexes, 35-base pairs in length, were generated in their A-forms by the 3DNA software.[25] The simulated dsRNA duplexes contained complementary strands, where the 5′ → 3′ strand had the sequence UAACAACCA-GAUCAAAGAAAAAACAGACAUUGUCA, as in our previous experiments.[19] DNA strands had sequences analogous to RNA strands, with the exception that U bases were replaced with T

bases. In the initial structures of complexes, TRBP-RBD2 was positioned approximately in the middle of the duplexes to avoid its interaction with duplex edges, as shown in Figure 1.

The *cionize* code, available as a VMD plugin,[26] was used to place Na^+ counterions neutralizing nucleic acid charges around the prepared duplexes and complexes. The resulting structures were solvated in TIP3P water and 50 mM NaCl with the VMD plugins *solvate* and *ionize*.[26] The final systems contained approximately 80 000 atoms (in the case of simulations involving duplexes) and 105 000 atoms (in the case of simulations involving protein and duplexes).

Molecular Dynamics Simulations. MD simulations were performed with NAMD2 software,[27] where the systems were described by assuming the AMBER force field with SB[28] and BSC0[29] corrections, a suitable choice for describing RNA.[30,31] The particle-mesh Ewald (PME) method[32] was used for evaluation of long-range Coulomb interactions. The time step was set to 1.0 fs, and long-range interactions were evaluated every 2 (van der Waals) and 4 timesteps (Coulombic). After 2000 steps of minimization, ions and water molecules were equilibrated for 2 ns around duplexes and complexes, which were constrained using harmonic forces with a spring constant of 1 kcal/(mol Å^2). Then, unconstrained duplexes and complexes were simulated for 50 and 100 ns, respectively. The simulations were performed in *NpT* ensemble, at a constant temperature T = 310 K, a Langevin constant γ_{Lang} = 1.0 ps^{-1}, and at a constant pressure p = 1 bar.

Data Analysis. To analyze the binding of TRBP-RBD2 to three duplexes, we computed the contact area a_{con} with dependence on time t, defined as

$$a_{con}(t) = \frac{a_{dsRBD}(t) + a_{dupl}(t) - a_{dsRBD:dupl}(t)}{2} \quad (1)$$

where a_{dsRBD}, a_{dupl}, and $a_{dsRBD:dupl}$ are the solvent accessible surface areas (SASA) of TRBP-RBD2, the nucleic acid duplex, and the TRBP-RBD2:duplex complex, respectively. The evaluation was done by the SASA built-in VMD plugin,[26] where the van der Waals radius of 1.4 Å was assigned to atoms to identify the points on a sphere that are accessible to the solvent. We also calculated the interaction energy between TRBP-RBD2 and each nucleic acid duplex by the NAMDenergy function in VMD.[26]

The forms of duplexes were analyzed from single averaged structures of duplexes and complexes. These averaged structures were obtained by averaging the coordinates of aligned duplexes and complexes over specified portions of trajectories. The helical rise values for nucleic acid duplexes, which characterize duplex forms, were evaluated with the 3DNA software.[25]

3. RESULTS

The fact that TRBP recognizes dsRNA over DNA−RNA and dsDNA has been established in previous experiments.[19−21,33] Here we examine through MD simulations and experiment how TRBP dsRBDs actually recognize dsRNA duplexes over nucleic acid duplexes that contain DNA.

TRBP-RBD2 Binding to Nucleic Acid Duplexes in EMSA Gels. To examine relative binding affinities of TRBP-RBD2 for dsRNA, DNA−RNA, and dsDNA duplexes, we performed electrophoretic mobility shift assays (EMSA) for solutions containing these duplexes and 0, 1, 3, or 10 μM TRBP-RBD2. The resulting EMSA gels, shown in Figure 2,

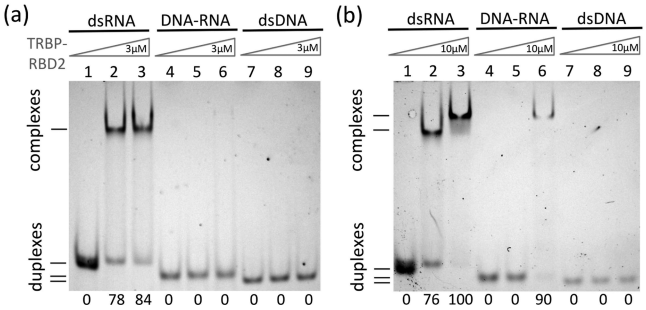

Figure 2. EMSA demonstrates that the binding affinity of TRBP-RBD2 is strongest for dsRNA, and weakest for dsDNA. (a) EMSA of 25-bp duplexes incubated with 0, 1, and 3 μM of TRBP-RBD2. TRBP-RBD2 binds to dsRNA and does not bind to DNA−RNA or dsDNA. (b) EMSA of 25-bp duplexes incubated with 0, 1, and 10 μM of TRBP-RBD2. TRBP binds to dsRNA and DNA:RNA (5−10 μM TRBP-RBD2, as shown in Figure S2, Supporting Information) and does not bind to dsDNA. The quantified binding fraction of TRBP-RBD2 to each duplex is displayed below the gel images.

contain strong upper bands in lines 2 and 3, indicating that TRBP-RBD2:dsRNA complexes are formed at 1, 3, and 10 μM TRBP-RBD2 concentrations. The fact that in Figure 2b the location of the upper band in line 3 is higher than in line 2 indicates that the number of bound TRBP-RBD2 molecules per dsRNA duplex increases with TRBP-RBD2 concentration. There is usually no relative affinity of dsRBDs for DNA−RNA and dsDNA reported in the literature.[19−21] Here, the EMSA gel in Figure 2b shows that 10 μM TRBP-RBD2 binds to DNA−RNA and does not bind to dsDNA. Therefore, TRBP-RBD2 has the greatest affinity for dsRNA, a smaller affinity for DNA−RNA, and no discernible affinity for dsDNA at the tested TRBP-RBD2 concentrations.

TRBP-RBD2 Binding to dsRNA in MD Simulations. In Figure 1a,b, we show a snapshot of TRBP-RBD2 in complex with a 35-base pair RNA duplex, based on the crystal structure of TRBP-RBD2 with coaxially stacked RNA duplexes.[24] TRBP-RBD2, a domain with the $\alpha\beta\beta\beta\alpha$ fold, binds to dsRNA along the duplex axis and across three grooves of the duplex (minor−major−minor grooves), similarly to other dsRBDs.[34−37] dsRNA minor grooves are lined with 2′-hydroxyl groups on sugar rings of RNA nucleotides, and the major grooves are lined with the negatively charged phosphate ($-PO_4^-$) groups. dsRNA duplex assumes the A-form, in which the widths of minor and major grooves are comparable (Figure 1a).

The contacts between TRBP-RBD2 and dsRNA are either direct (hydrogen bonding) or water-mediated (hydrogen bonding through water molecules that have long residence times). Bases of the minor groove I contact polar (His159, Gln165) and negatively charged (Glu166) residues, and bases of the minor groove II contact polar (His188) and positively charged (Arg189, Lys190) residues (Figure 1b). The $-PO_4^-$ groups of the dsRNA major groove contact polar (Thr208) and positively charged (Lys210, Lys211, Lys214, Arg215) residues of helix α_2, which lies across the width of the major groove.

In Figure 1c, we compare the sequences of two RBDs in TRBP. Interestingly, not all the residues, which contribute to binding of TRBP-RBD2 to dsRNA, are conserved: Glu166, His188, Lys210, Lys211, and Lys214 are conserved, whereas Gln165, Arg189, Lys190, and Arg215 are not conserved.

TRBP-RBD2 Binding to Noncognate Substrates. Next, we examine the binding of TRBP-RBD2 to nucleic acid

duplexes containing DNA. Snapshots of TRBP-RBD2 in complex with DNA−RNA and dsDNA, captured at the end of 100 ns long simulations, are shown in Figure 3a,b,

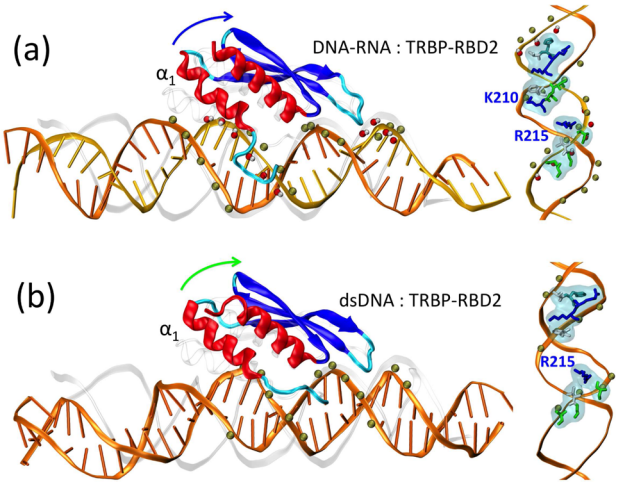

Figure 3. Binding of TRBP-RBD2 to noncognate duplexes: (a) DNA−RNA hybrid and (b) dsDNA. RNA strands are shown in gold and DNA strands in orange. For comparison, the TRBP-RBD2:dsRNA complex is shown in transparent ribbon representation with protein and RNA backbones aligned to the backbones of the complexes shown in color. Curved arrows mark displacements of α_1 helices of TRBP-RBD2 in complexes with DNA−RNA and dsDNA, as compared to complexes with dsRNA. Top views of binding interfaces are shown on the right, where TRBP-RBD2 residues within 3 Å of duplexes are highlighted in both transparent surface and licorice representations. The residues are colored according to residue type, as described in Figure 1b.

respectively. For comparison, the TRBP-RBD2:dsRNA complex is overlaid as a shadow. Even though the simulations were started with DNA−RNA and dsDNA duplexes in A-forms, these duplexes changed to B-forms within several nanoseconds of the simulations; in MD simulations with the selected force field,[29] free dsDNA duplexes assume B-forms[38] and free dsRNA duplexes assume A-forms,[30] in agreement with experimental data. Quick (≈1 ns) A → B form changes of DNA strands in dsDNA and DNA:RNA duplexes were observed and characterized in previous short scale simulations.[39] After 100 ns of equilibration, DNA−RNA and dsDNA duplexes are significantly longer than dsRNA, despite all duplexes having the same number of base pairs. During simulations, DNA−RNA and dsDNA relaxed to forms with significantly wider major grooves and narrower minor grooves, thus departing from their initial A-forms. Analyses of selected helical parameters (Table S1, Supporting Information), including twist, slide, and roll, show that DNA−RNA and dsDNA duplexes in complex with TRBP-RBD2 are distinctly non-A-form and are similar in form to free duplexes.[39,40] In addition, Table S1 (Supporting Information) shows that DNA strands of DNA−RNA and dsDNA duplexes acquire dihedral angles (δ, ϵ) and phase angles of pseudorotation (P) characteristic of DNA strands in B-form, comparable to values reported in ref 40.

Results in Figures 1b and 3 show that DNA−RNA and dsDNA duplexes stay in contact with a smaller number of TRBP-RBD2 residues than does dsRNA. Binding of TRBP-RBD2 to minor groove I is significant only for the dsRNA duplex, where helix α_1 lies across the minor groove I and remains in close contact with it. Minor grooves I of DNA−RNA and dsDNA are more exposed to solvent, because helix α_1 is lifted from the groove. Binding of TRBP-RBD2 to major grooves is also more prominent for dsRNA. The numbers of TRBP-RBD2 contacts to the minor groove II are very similar for all three studied duplexes.

Parts a and c of Figure 4 show contact areas and interaction energies of TRBP-RBD2 and three duplexes, evaluated during the last 85 ns of the simulations. The contact area decreases (Figure 4a) and binding energy becomes less favorable (Figure 4c) as the DNA content of the duplex increases. The number of hydrogen bonds between TRBP-RBD2 and three duplexes also

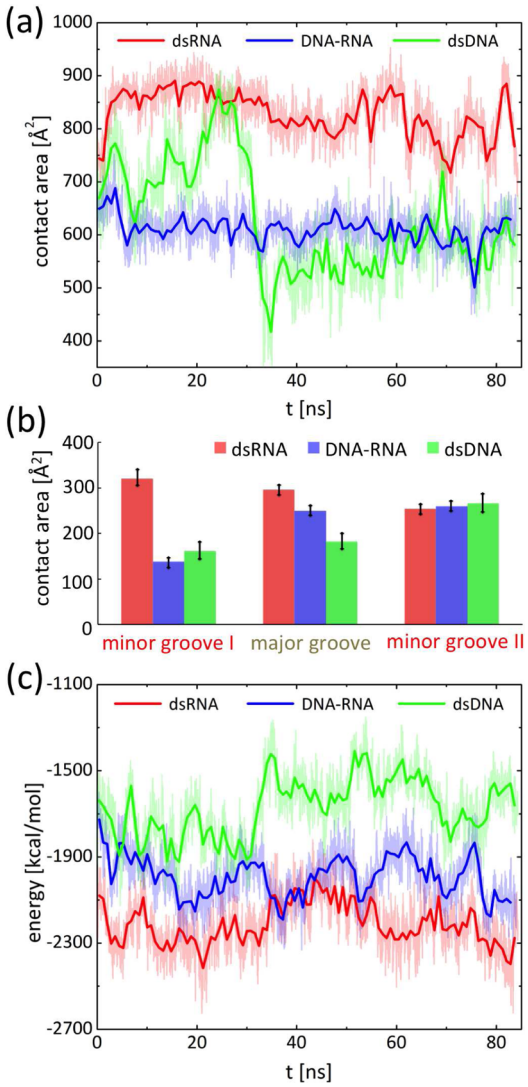

Figure 4. Interaction of TRBP-RBD2 with three duplex types. (a) Contact areas between TRBP-RBD2 and dsRNA, DNA−RNA, and dsDNA. (b) Contact areas between TRBP-RBD2 and individual nucleic acid grooves (minor grooves I and II, major groove, marked in Figure 1a). Contact areas were measured between whole duplexes and sets of the TRBP-RBD2 residues above the selected grooves, H159, E160, V161, G162, A163, Q165, E166, V168, V169, Q170, R174, L175, Y178 (for minor groove I); F192, T208, S209, K210, K211, L212, K214, R215 (major groove); E183, P186, A187, H188, R189, K190, E191 (minor groove II). (c) Interaction (nonbonding) energy between TRBP-RBD2 and the three duplexes. The plots are shown for the last 85 ns of trajectories. In (a) and (c) thin lines correspond to data sampled from trajectories and thick lines show gliding time averages over 800 ps.

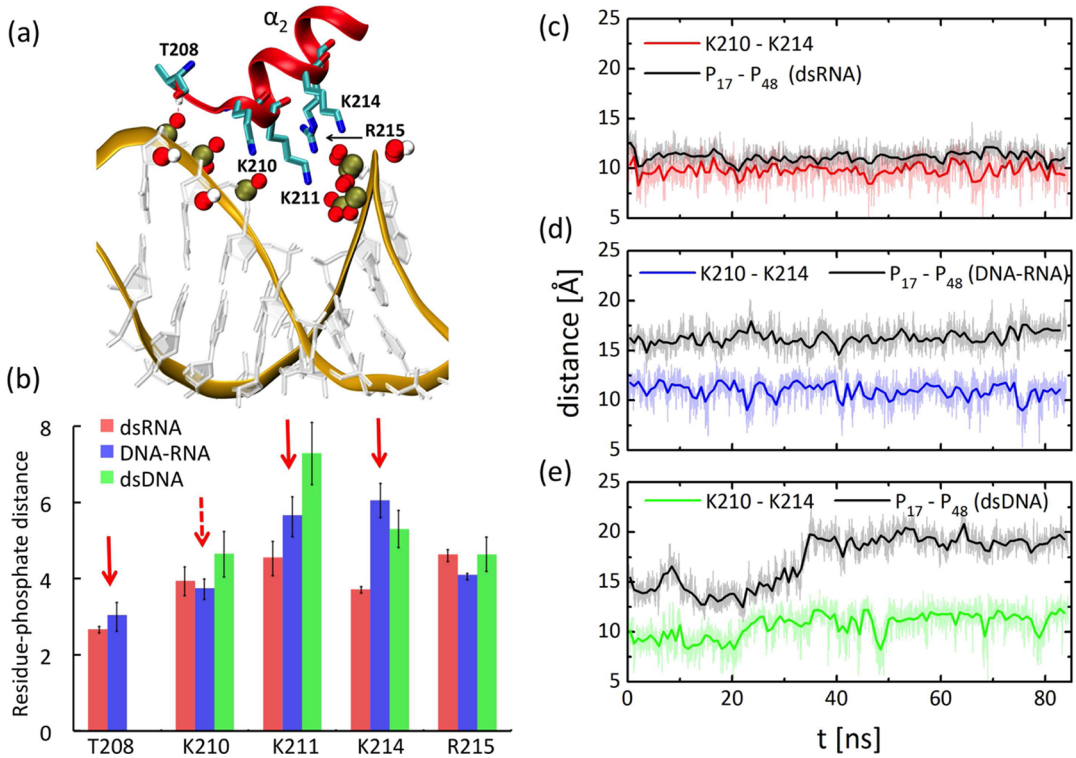

Figure 5. Major groove interactions. (a) Binding of TRBP-RBD2 to the major groove of dsRNA. The residues that interact through Coulomb interactions (Lys and Arg) and hydrogen bonding (Thr) are highlighted, together with their bonding partners, negatively charged phosphate groups. Oxygen, hydrogen, and phosphorus atoms are shown as red, white, and tan spheres, respectively, carbon and nitrogen are shown in cyan and blue. (b) Average distances of TRBP-RBD2 residues from the phosphate groups nearest to them (phosphorus atoms for Lys and Arg, and oxygen atom for Thr208), averaged over the last 80 ns of simulations. Red arrows mark the residues that bind to dsRNA more tightly than to DNA−RNA or dsDNA. Register fit of the Lys210−Lys214 pair in major grooves of dsRNA (c), DNA−RNA (d), and dsDNA (e). Lys210−Lys214 distances and the distances between two phosphate groups that coordinate Lys210 and Lys214 are shown. These distances are calculated between phosphate atoms of RNA nucleotides 17 and 48, and between nitrogen atoms of Lys210 and Lys214 side chains. The distance between P_{17} and P_{48} characterizes the major groove width of the duplexes. In (c)−(e) thin lines correspond to data sampled from trajectories and thick lines show gliding time averages over 800 ps.

decreases with the increase of DNA content (Figure S3, Supporting Information), confirming that TRBP-RBD2 binds most favorably to its cognate substrate, dsRNA, in agreement with our experiments.

The individual contributions to the net contact area are shown for each (minor−major−minor) groove in Figure 4b. These contact areas were evaluated between whole duplexes and selected groups of TRBP-RBD2 amino acid residues directly above each of the grooves. The results confirm that TRBP-RBD2 has much less contact with the minor groove I in case of DNA-containing duplexes than in case of the dsRNA duplex; the contact area between TRBP-RBD2 and DNA−RNA or dsDNA minor grooves I is only ≈40−50% of the contact area between TRBP-RBD2 and dsRNA minor groove I. The contact area between TRBP-RBD2 and the duplex major groove also decreases with the increased DNA content of the duplex. The results indicate that TRBP-RBD2 recognizes dsRNA on the basis of interactions in minor groove I and in the major groove.

TRBP-RBD2 Recognizes dsRNA- over DNA-Containing Substrates. *Recognition at the Major Groove.* The binding mode of TRBP-RBD2 to the major groove of dsRNA is shown in Figure 5a. Five amino acid residues, Thr208, Lys210, Lys211, Lys214, and Arg215, make direct contact with the dsRNA backbone at the major groove. Thr208, Lys210, Lys214, and Arg215 bind to the parts of the dsRNA major groove directly beneath them. On the other hand, Lys211 lies across the major groove. Its backbone atoms are on one side of the groove, whereas its positively charged tip contacts the $-PO_4^-$ group on the opposite side of the major groove.

The stability of binding between the five identified residues to major grooves of dsRNA, DNA−RNA, and dsDNA is examined by tracking distances of these residues to their nearest neighbor $-PO_4^-$ groups. In Figure 5b, we show these distances averaged over the last 85 ns of trajectories (time evolution of these distances is shown in Figure S4, Supporting Information). The results show that Thr208 makes a hydrogen bond to the nearest $-PO_4^-$ group in dsRNA and DNA−RNA duplexes but does not engage in hydrogen bonding in case of the dsDNA duplex. The distances between Lys210 and Arg215 to the nearest $-PO_4^-$ groups are similar for all three duplexes, but the distances between Lys211 and Lys214 to the nearest $-PO_4^-$ groups are perturbed when the duplex contains DNA, involving a gradual increase in the average distance of Lys211 to the nearest $-PO_4^-$ group with the increase of DNA content in the duplex. Likewise, the distance between Lys214 to the nearest $-PO_4^-$ group becomes longer and less stable for DNA-containing duplexes.

Although the results in Figure 5b show that Lys211 and Lys214 enable TRBP-RBD2 to recognize and bind to dsRNA, experiments have shown that single mutations of His188, Lys210, and Lys214 block TRBP-RBD2 binding to dsRNA.[13] A

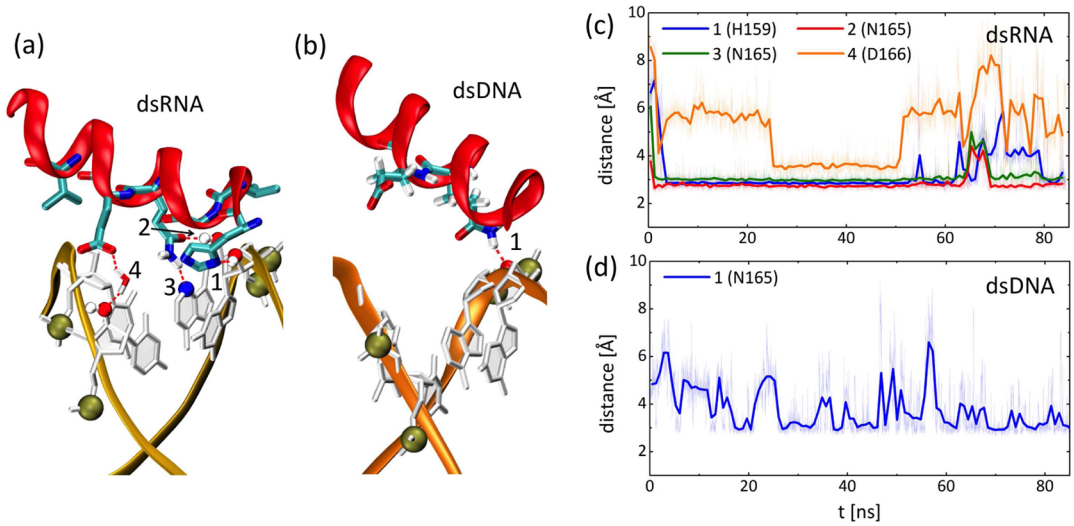

Figure 6. Interactions of TRBP-RBD2 residues with minor grooves I of (a) dsRNA and (b) dsDNA. (c) Time dependent distances of stable contacts between TRBP-RBD2 and dsRNA minor groove I. (d) Same as in (c) for TRBP-RBD2 and dsDNA minor groove I. In (d) thin lines correspond to data sampled from trajectories and thick lines show gliding time averages over 800 ps.

closer look at the binding mode of TRBP-RBD2 and the dsRNA major groove indicates that Lys210 and Lys214 form a pair that bridges $-PO_4^-$ groups on two sides of the dsRNA major groove. In Figure 5c–e, we analyze the distances between Lys210 and Lys214, and between $-PO_4^-$ groups that coordinate them (the distances are measured between the nitrogen atoms of Lys210 and Lys214 side chains, and between the phosphate atoms of RNA nucleotides 17 and 48, respectively). The results show evidence for a "register" fit of Lys210–Lys214, as the lysine pair fits exactly above the $-PO_4^-$ groups that coordinate them. The distance between positively charged tips of Lys210 and Lys214 residues is always in the range ≈9–13 Å, whereas the distance between the bridging $-PO_4^-$ groups increases from ≈11 Å for dsRNA to ≈17 Å for DNA–RNA and to ≈20 Å for dsDNA. Therefore, the Lys210-Lys214 pair fits poorly in the major grooves of DNA–RNA and dsDNA duplexes because the major grooves of these duplexes are significantly wider, as shown in Figure S5 (Supporting Information). Similarly, Lys211 cannot effectively bridge the 17–20 Å distance across the major groove of DNA–RNA and dsDNA.

Recognition at Minor Grooves. dsRBDs bind to two minor grooves of dsRNA,[24,34–37] in the binding mode shown in Figure 1a. Minor grooves of dsRNA are lined with 2′-hydroxyl (OH) groups, located on the sugar rings of RNA bases. However, DNA bases lack 2′-hydroxyl groups. To explore the effect of the 2′-OH groups on dsRBD binding to three duplexes, we analyze the dsRBD binding to minor grooves I and II.

Snapshots of TRBP-RBD2 bound to minor grooves I of dsRNA and dsDNA are shown in Figure 6a,b. When TRBP-RBD2 binds to dsRNA, its α_1-helix extends across the groove. His159 and Gln165 residues of the α_1-helix make three direct hydrogen bonds to dsRNA, and Glu166 makes one water-mediated bond. The three direct hydrogen bonds remain stable for most of the time during the last 85 ns of the trajectory, whereas the water-mediated bond exhibits significant fluctuation (Figure 6c). On the other hand, TRBP-RBD2 does not bind across the minor groove I of dsDNA. Figure 6b,d shows that for this complex only Gln165 makes a hydrogen bond to the phosphate group of the nearest DNA nucleotide, albeit only a fluctuating one. Binding of TRBP-RBD2 to DNA–RNA is very similar to its binding to dsDNA (not shown).

Figure 6a,b demonstrates that minor grooves I of dsRNA and dsDNA have different forms: the minor groove I of dsRNA is wide and shallow (A-form like), with its bases being in contact with TRBP-RBD2 helix α_1, whereas minor groove I of dsDNA is narrower and much deeper (B-form like), with its bases being buried below the α_1 helix. The results in Figure 6 show clearly that the A-form of the minor groove I facilitates TRBP-RBD2 binding.

TRBP-RBD2 exhibits a binding (contact) area to minor groove II that is similar for all three duplexes (Figure 4b). However, the binding modes in this groove differ between the three duplexes. For TRBP-RBD2 bound to dsRNA minor groove II, the His188 hydrogen binds to the 2′-OH group, whereas Arg189 and Lys190 occasionally interact with the 2′-OH groups or the backbone phosphate groups. For TRBP-RBD2 bound to DNA–RNA minor groove II, His188 is unbound, whereas Arg189 and Lys190 form stable hydrogen bonds to two bases. Lastly, for TRBP-RBD2 bound to dsDNA, His188 makes a hydrogen bond to one of the bases, whereas Arg189 and Lys190 bind Coulombically to the negatively charged backbone phosphate groups. Because Arg189 and Lys190 residues are not conserved, dsRBDs without these residues would exhibit weaker binding to the minor groove II of DNA-containing duplexes.

Duplex Form at the TRBP-RBD2 Binding Site. Results in Figures 5 and 7 already show that the duplex form with its minor and major grooves plays a significant role in optimal TRBP-RBD2 binding. Here, we examine the complete duplex forms at the sites of binding to TRBP-RBD2. To compare in this regard the dsRNA, DNA–RNA, and dsDNA duplex forms at TRBP-RBD2 binding sites, single average structures of the respective complexes were characterized by considering structures averaged over the last 40 ns of trajectories and then aligning the TRBP-RBD2 domains of these structures.

The resulting duplexes at the binding site are shown in Figure 7a. Several structural features can be clearly discerned. First, the width of the major groove is narrowest for dsRNA,

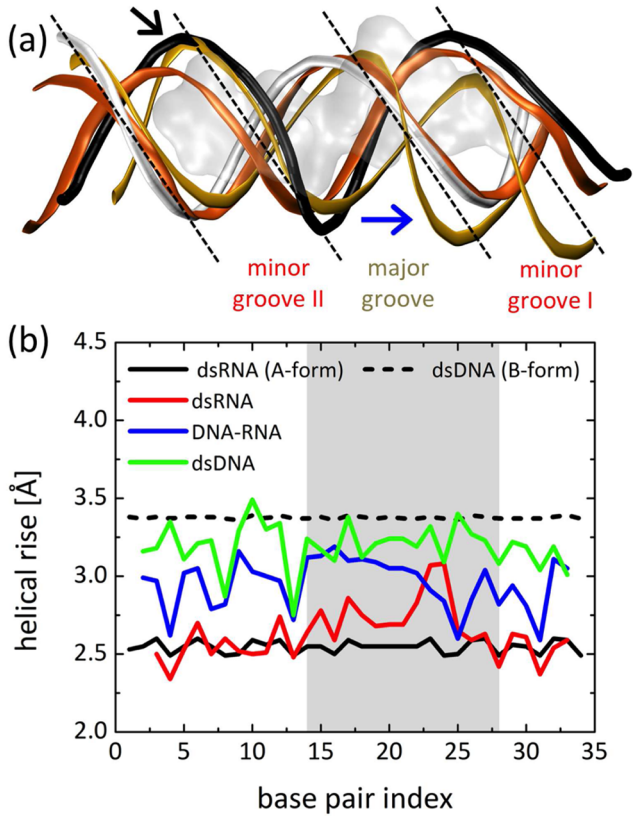

Figure 7. Duplex forms at TRBP-RBD2 binding sites. The structures of complexes analyzed in (a) and (b) are obtained by averaging the coordinates of each system over the last 40 ns of simulation. (a) Duplex backbones at TRBP-RBD2 binding sites. dsRNA strands are shown in gold, dsDNA strands are shown in orange, and strands of the DNA−RNA hybrid are shown as black (DNA) and white (RNA) tubes. TRBP-RBD2 domains, bound to the shown duplexes, are aligned. The shaded area outlines the TRBP-RBD2 residues in contact with the dsRNA duplex (within 3.0 Å of it). The minor−major−minor groove pattern is labeled and highlighted by the black dashed lines. Arrows point to major differences in duplex forms in binding regions. (b) Helical rise for duplex base pairs of A-form dsRNA, B-form dsDNA, and averaged structures of dsRNA, DNA−RNA, and dsDNA bound to TRBP-RBD2. The shaded region of the graph marks the base pairs that form the binding site for TRBP-RBD2. A- and B-form structures are generated with 3-DNA software.[25]

wider for DNA−RNA, and widest for dsDNA. The increase in the major groove width with the increased DNA content is the reason for the gradual decrease of TRBP-RBD2 binding to the major groove of the three duplexes (Figure 4b). Second, minor grooves I of DNA−RNA and dsDNA can be almost perfectly superimposed on each other, but not to the more compressed minor groove I of dsRNA; only dsRNA achieves stable binding to TRBP-RBD2. Third, the minor groove II of DNA−RNA assumes a form almost identical to that of dsRNA, whereas dsDNA exhibits a much narrower minor groove II.

When DNA−RNA is simulated without bound TRBP-RBD2, both of its minor grooves resemble closely the dsDNA minor grooves (Figure S6b, Supporting Information). Therefore, through the presence of TRBP-RBD2, the minor grooves of DNA−RNA adopt either dsRNA or dsDNA forms, depending on the interactions with the protein (Figure S5b, Supporting Information). Similar duplex flexibility and duplex adaptation to bound proteins has been observed for dsDNA duplexes.[41] Interestingly, it is the DNA strand of the DNA−RNA minor groove II that changes its conformation and is almost perfectly overlaid with the RNA strand of the dsRNA, as shown in Figure 7a.

In Figure 7b, we compare the helical rise of the duplexes simulated with bound TRBP-RBD2. The helical rise is the distance between neighboring bases in the duplex helix. For perfect A-form dsRNA it is ≈2.5 Å, whereas for B-form dsDNA it is 3.4 Å. For duplexes bound to TRBP-RBD2, the helical rise is evaluated for the averaged structures. The results show for dsRNA a perfect A-form, except in one region of widened major groove (experimentally confirmed for dsRBDs[34]). For DNA−RNA, the helical rise is between A- and B-forms, as observed in other studies of free DNA−RNA duplexes;[39,40] for dsDNA the helical rise is again between A- and B-form, but very close to the B-form value. dsRNA has the smallest helical rise and remains closest to the A-form.

In Table S1 (Supporting Information), we further quantify forms of duplexes bound to TRBP-RBD2 and list their selected average helical parameters (twist, slide, roll), as well as dihedral angles (δ, ϵ) and phase angles of pseudorotation (P). Comparison of Table S1 (Supporting Information) to parameters of free duplexes[40] shows that free and dsRBD-bound duplexes have similar forms. Overall, DNA strands in dsDNA and DNA−RNA duplexes have parameters characteristic of the B-form, whereas RNA strands in dsRNA and DNA−RNA have parameters characteristic of the A-form. However, dihedral angles δ and phase angles P of DNA nucleotides in TRBP-RBD2:DNA−RNA complex, shown in Figure S8 (Supporting Information), show that DNA nucleotides can switch to the A-form when bound to TRBP-RBD2.

4. DISCUSSION

In the present article, we have clarified by means of MD simulations the experimental observation that dsRBDs recognize and bind to dsRNA and avoid binding to similar DNA−RNA and dsDNA duplexes. Previous experiments showed that isolated first and second dsRBDs of TRBP bind stably to dsRNA, with binding affinities of 220 and 110 nM, respectively.[42] Our experiments, shown in Figure 2, confirmed that TRBP-RBD2 (1−10 μM) binds to dsRNA. In agreement with experiments, MD simulations showed that TRBP dsRBDs bind stably to dsRNA, with the second dsRBD having a more favorable interaction energy with dsRNA than the first dsRBD (Figure S9, Supporting Information).

Although there are examples of domains and proteins that can bind to both RNA and DNA,[43−46] TRBP and other dsRBD-containing proteins do not bind well to DNA−RNA and dsDNA duplexes.[19−21] For example, dsRBDs of PKR bind to dsRNA and DNA−RNA with K_d = 0.17 μM and ≥500 μM, respectively, whereas no binding to dsDNA was observed in the tested experimental conditions.[21] The whole TRBP protein (10 nM to 2 μM concentration) binds to dsRNA, but not to DNA−RNA and dsDNA.[19,20] However, some dsRBD proteins, such as 4F protein that contains two dsRBDs, can bind strongly to both dsRNA and DNA−RNA duplexes; DNA−RNA duplexes at 50 pM concentration were able to compete with dsRNA duplexes for binding to 4F.[22] Our experimental results in Figure 2 show that at the concentration of 5−10 μM, TRBP-RBD2 binds to 20−90% of the present DNA−RNA and does not bind to dsDNA. Therefore, TRBP-RBD2 can discriminate between dsRNA and DNA−RNA more effectively than 4F and less effectively than PKR. In agreement with the experimental results, complexes of TRBP-RBD2 with DNA−RNA and

dsDNA were less stable in the performed MD simulations than complexes with dsRNA, as shown in Figures 1, 3, and 4.

MD simulations reveal that the duplex form plays an important role in the recognition of dsRNA- over DNA-containing duplexes by dsRBDs, as has already been hypothesized on the basis of dsRBD:dsRNA complex structures.[5] A proper binding of a dsRBD to a nucleic acid duplex is determined by a proper "register fit" of the dsRBD into three successive duplex grooves, which is in turn largely determined by the duplex form. Though dsRNA duplex has the A-form, DNA-containing duplexes quickly adopt an intermediate form (DNA−RNA) and the B-form (dsDNA), as seen in Figures 7 and S6 (Supporting Information). By adopting B-like forms, DNA-containing duplexes have wider major grooves and narrower minor grooves than dsRNA. For example, the major grooves of DNA-containing duplexes become 6−9 Å wider than the major groove of dsRNA (Figure 5c−e).

As a result of changed forms, binding of TRBP-RBD2 to DNA−RNA and dsDNA becomes significantly impaired in major grooves and in minor grooves I, but not in the minor groove II, as quantified in Figure 4b. Delayed changes of the dsDNA major groove width at the binding site, seen in Figure 5e, show the importance of the duplex form for dsRBD binding. Preserved contacts between the dsDNA major groove and three basic residues, Lys 210, Lys 211, and Lys 214, keep dsDNA from adopting its preferred major groove width during the first 50 ns of simulations. In comparison, dsDNA without the bound dsRBD adopts very quickly wide major grooves of the B-form. Similarly, TRBP-RBD2 easily contacts the bases in the wide and shallow minor groove I of dsRNA but cannot contact the bases in the deeper and narrower minor groove I of dsDNA (Figure 6). In principle, dsRBDs could bind dsDNA if dsDNA was flexible enough to adopt the A-form. However, although B-form DNA was shown to be highly flexible, its distortions do not necessarily change its global helical conformation.[47] Otherwise, dsRBDs could bind DNA-containing duplexes if dsRBDs were flexible and able to structurally conform to these duplexes. However, the simulations show that dsRBDs resist structural changes in the presence of dsDNA and DNA−RNA and validate previous hypotheses and observations on dsRBD rigidity.[5]

The contribution of 2′-OH groups to binding of dsRBDs to dsRNA was previously examined for PKR, a protein with two dsRBDs, binding to chimeric dsRNA duplexes with several 2′-OH groups substituted to 2′-H or 2′-OCH_3.[21] Several results indicated that 2′-OH groups play a more important role than the duplex form in PKR binding to dsRNA. For example, only one ionic contact was found between PKR and dsRNA, and the mutagenesis studies showed that one Lys residue is required for PKR:dsRNA binding (Lys 60 in PKR-RBD1, analogous to Lys 210 in TRBP-RBD2).[48] However, more recently, crystal structures of dsRBD:dsRNA complexes identified multiple ionic interactions between dsRBDs and dsRNA phosphate groups.[24,34] Mutagenesis studies of TRBP showed that three residues of TRBP-RBD2, His 188, Lys 210, and Lys 214, are required for TRBP-RBD2 binding to dsRNA.[13] Smaller involvement of ionic interactions between PKR and dsRNA could be due to PKR lacking several basic residues that contribute to strong binding of TRBP-RBD2 to dsRNA and its major groove. PKR-RBD1 lacks the residues analogous to Arg 190 and Arg 215 of TRBP-RBD2, whereas PKR-RBD2 lacks the residues analogous to Arg 190, Lys 191, Lys 211, and Arg 215 of TRBP-RBD2.[5] The observation that the Lys 210 and Lys 214 pair of TRBP-RBD2 has to fit well into the major groove of the duplex for the dsRBD to bind stably to the duplex, as shown in Figure 5 (c-e), highlights the importance of shape on binding of dsRBDs to duplexes.

Although dsRBDs are known to not bind to DNA−RNA and dsDNA,[19−21] experimental results in Figures 2 and S2 (Supporting Information) show that TRBP-RBD2 at concentration >5 μM has a higher binding affinity for DNA−RNA than for dsDNA. The higher affinity of TRBP-RBD2 for DNA−RNA is likely due to the narrower major groove of DNA−RNA (Figure 5d) and the fact that TRBP-RBD2 can alter the width of DNA−RNA grooves and strengthen the binding. The latter was observed in the minor groove II of the DNA−RNA duplex, which acquired the width of an A-form duplex, due to DNA nucleotides changing from B- to A-form conformations (Figure S8, Supporting Information) upon binding to TRBP-RBD2 (Figure S7b, Supporting Information). The observed B- → A-form change of DNA nucleotides and the resulting minor groove width modulation potentially explain how other dsRBD proteins, such as 4F,[22] can also bind to DNA−RNA hybrids.

In the present article we have shown how dsRNA binding proteins distinguish between dsRNA- and DNA-containing duplexes. Additional studies are needed to explain the observed sequence specific binding of other dsRNA binding proteins,[5,36,49] and to understand dsRBD binding to dsRNA with mismatches, small bulges and loops, common in microRNA (miRNA) in the silencing by RNA interference pathways.[15,16]

■ ASSOCIATED CONTENT

Supporting Information

SEQLOGO constructed from 8 sequences of dsRBDs. EMSA of 25-bp duplexes incubated with 0, 1, and 5 μM of TRBP-RBD2. Time dependence of the number of hydrogen bonds between TRBP-RBD2 and the studied duplexes. A table of averages for selected helical parameters. Time dependence of distances between the positively charged TRBP-RBD2 residues and phosphate groups of the studied duplexes. Register fit of Lys210−Lys214 pair in major grooves of dsRNA, DNA−RNA, and dsDNA. Duplex forms of dsRNA, DNA−RNA, and dsDNA. Duplex forms at TRBP-RBD2 binding sites for the studied duplexes. Dihedral δ and phase angle P for DNA nucleotides of DNA−RNA duplex. Contact area and interaction energy between TRBP-RBD1 and and TRBP-RBD2 with dsRNA. This material is available free of charge via the Internet at http://pubs.acs.org

■ AUTHOR INFORMATION

Corresponding Authors

*L. Vuković: e-mail, lvukov1@illinois.edu.
*S. Myong: e-mail, smyong@illinois.edu.
*K. Schulten: e-mail, kschulte@ks.uiuc.edu.

Funding

National Science Foundation (grant NSF-PHY-0822613) and National Institutes of Health (grants NIH 9P41GM104601 and 1DP2GM105453).

Notes

The authors declare no competing financial interest.

■ ACKNOWLEDGMENTS

This work was supported by the National Science Foundation grant NSF-PHY-0822613, the National Institutes of Health grant NIH 9P41GM104601 (K.S.), and an NIH Director's new

Innovator Award NIH 1DP2GM105453 (S.M.). We acknowledge computer time provided by the Texas Advanced Computing Center (XSEDE allocation MCB130078 to S. M.) and by the Computational Science and Engineering Program at the University of Illinois (Taub computing cluster). L.V. acknowledges support as a Center for the Physics of Living Cells (CPLC) Postdoctoral Fellow.

■ ABBREVIATIONS

dsRNA, double-stranded RNA; dsRBD, dsRNA binding domain; TRBP, transactivation response RNA binding protein; PKR, protein kinase R; RHA, RNA helicase A; ADAR, adenosine deaminase acting on RNA; PACT, protein activator of PKR; MD, molecular dynamics; EMSA, electrophoretic mobility shift assay; bp, base pair; TRBP-RBD2, second dsRBD of TRBP; PME, particle-mesh Ewald; SASA, solvent accessible surface area; TRBP-RBD1, first dsRBD of TRBP

■ REFERENCES

(1) Carpenter, S., Aiello, D., Atianand, M. K., Ricci, E. P., Gandhi, P., Hall, L. L., Byron, M., Monks, B., Henry-Bezy, M., Lawrence, J. B., O'Neill, L. A. J., Moore, M. J., Caffrey, D. R., and Fitzgerald, K. A. (2013) A long noncoding RNA mediates both activation and repression of immune response genes. *Science 341*, 789−792.

(2) Hansen, T. B., Jensen, T. I., Clausen, B. H., Bramsen, J. B., Finsen, B., Damgaard, C. K., and Kjems, J. (2013) Natural RNA circles function as efficient microRNA sponges. *Nature 495*, 384−388.

(3) Han, B.-W., and Chen, Y.-Q. (2013) Potential pathological and functional links between long noncoding RNAs and hematopoiesis. *Sci. Signal. 6*, 5.

(4) Bartel, D. P. (2009) MicroRNAs: Target recognition and regulatory functions. *Cell 136*, 215−233.

(5) Masliah, G., Barraud, P., and Allain, F. H.-T. (2012) RNA recognition by double-stranded RNA binding domains: a matter of shape and sequence. *Cell. Mol. Life Sci. 70*, 1875−1895.

(6) Tian, B., Bevilacqua, P. C., Diegelman-Parente, A., and Mathews, M. B. (2004) The double-stranded-RNA-binding motif: interference and much more. *Nat. Rev. Mol. Cell Biol. 5*, 1013−1023.

(7) Saunders, L. R., and Barber, G. N. (2003) The dsRNA binding protein family: critical roles, diverse cellular functions. *FASEB J. 17*, 961−983.

(8) Nanduri, S., Carpick, B. W., Yang, Y., Williams, B. R., and Qin, J. (1998) Structure of the double-stranded RNA-binding domain of the protein kinase PKR reveals the molecular basis of its dsRNA-mediated activation. *EMBO J. 17*, 5458−5465.

(9) Lee, C.-G., and Hurwitz, J. (1992) A new RNA helicase isolated from HeLa cells that catalytically translocates in the 3′ to 5′direction. *J. Biol. Chem. 267*, 4398−4407.

(10) Zhang, H., Kolb, F. A., Brondani, V., Billy, E., and Filipowicz, W. (2002) Human Dicer preferentially cleaves dsRNAs at their termini without a requirement for ATP. *EMBO J. 21*, 5875−5885.

(11) Wostenberg, C., Lary, J. W., Sahu, D., Acevedo, R., Quarles, K. A., Cole, J. L., and Showalter, S. A. (2012) The role of human Dicer-dsRBD in processing small regulatory RNAs. *PLoS One 7*, e51829.

(12) Knight, S. W., and Bass, B. L. (2002) The role of RNA editing by ADARs in RNAi. *Mol. Cell 10*, 809−817.

(13) Daniels, S. M., and Gatignol, A. (2012) The multiple functions of TRBP, at the hub of cell responses to viruses, stress, and cancer. *Microbiol. Mol. Biol. R. 76*, 652−666.

(14) Kok, K. H., Ng, M.-H. J., Ching, Y.-P., and Jin, D.-Y. (2007) Human TRBP and PACT directly interact with each other and associate with Dicer to facilitate the production of small interfering RNA. *J. Biol. Chem. 282*, 17649−17657.

(15) Noland, C. L., and Doudna, J. A. (2013) Multiple sensors ensure guide strand selection in human RNAi pathways. *RNA 5*, 639−648.

(16) Lee, H. Y., Zhou, K., Smith, A. M., Noland, C. L., and Doudna, J. A. (2013) Differential roles of human Dicer-binding proteins TRBP and PACT in small RNA processing. *Nucleic Acids Res. 41*, 6568−6576.

(17) Wilson, R. C., and Doudna, J. A. (2013) Molecular mechanisms of RNA interference. *Annu. Rev. Biophys. 42*, 217−239.

(18) Taylor, D. W., Ma, E., Shigematsu, H., Cianfrocco, M. A., Noland, C. L., Nagayama, K., Nogales, E., Doudna, J. A., and Wang, H.-W. (2013) Substrate-specific structural rearrangements of human Dicer. *Nat. Struct. Mol. Biol. 20*, 662−670.

(19) Koh, H. R., Kidwell, M. A., Ragunathan, K., Doudna, J. A., and Myong, S. (2013) ATP-independent diffusion of double-stranded RNA binding proteins. *Proc. Natl. Acad. Sci. U. S. A. 110*, 151−156.

(20) Gredell, J. A., Dittmer, M. J., Wu, M., Chan, C., and P, W. S. (2010) Recognition of siRNA asymmetry by TAR RNA binding protein. *Biochemistry 49*, 3148−3155.

(21) Bevilacqua, P. C., and Cech, T. R. (1996) Minor-groove recognition of double-stranded RNA by the double-stranded RNA-binding domain from the RNA-activated protein kinase PKR. *Biochemistry 35*, 9983−9994.

(22) Bass, B. L., Hurst, S. R., and Singer, J. D. (1994) Binding properties of newly identified Xenopus proteins containing dsRNA-binding motifs. *Curr. Biol. 4*, 301−314.

(23) Castrignano, T., Chillemi, G., Varani, G., and Desideri, A. (2002) Molecular dynamics simulation of the RNA complex of a double-stranded RNA-binding domain reveals dynamic features of the intermolecular interface and its hydration. *Biophys. J. 83*, 3542−3552.

(24) Yang, S. W., Chen, H.-Y., Yang, J., Machida, S., Chua, N.-H., and Yuan, Y. A. (2010) Structure of Arabidopsis HYPONASTIC LEAVES1 and its molecular implications for miRNA processing. *Structure 18*, 594−605.

(25) Lu, X.-J., and Olson, W. K. (2003) 3DNA: A software package for the analysis, rebuilding and visualization of three-dimensional nucleic acid structures. *Nucleic Acids Res. 31*, 5108−5121.

(26) Humphrey, W., Dalke, A., and Schulten, K. (1996) VMD: Visual molecular dynamics. *J. Mol. Graphics 14*, 33−38.

(27) Phillips, J. C., Braun, R., Wang, W., Gumbart, J., Tajkhorshid, E., Villa, E., Chipot, C., Skeel, R. D., Kalé, L., and Schulten, K. (2005) Scalable molecular dynamics with NAMD. *J. Comput. Chem. 26*, 1781−1802.

(28) Hornak, V., Abel, R., Okur, A., Strockbine, B., Roitberg, A., and Simmerling, C. (2006) Comparison of multiple Amber force fields and development of improved protein backbone parameters. *Proteins 65*, 712−725.

(29) Perez, A., Marchan, I., Svozil, D., Sponer, J., Cheatham, T. E., III, Laughton, C. A., and Orozco, M. (2007) Refinement of the AMBER force field for nucleic acids: Improving the description of α/γ conformers. *Biophys. J. 92*, 3817−3829.

(30) Besseova, I., Otyepka, M., Reblova, K., and Sponer, J. (2009) Dependence of A-RNA simulations on the choice of the force field and salt strength. *Phys. Chem. Chem. Phys. 11*, 10701−10711.

(31) Jung, S., and Schlick, T. (2014) Interconversion between parallel and antiparallel conformations of a 4H RNA junction in domain 3 of foot-and-mouth disease virus IRES captured by dynamics simulations. *Biophys. J. 106*, 447−458.

(32) Darden, T., York, D., and Pedersen, L. (1993) Particle mesh Ewald: An N · log(N) method for Ewald sums in large systems. *J. Chem. Phys. 98*, 10089−10092.

(33) Parker, G. S., Maity, T. S., and Bass, B. L. (2008) dsRNA binding properties of RDE-4 and TRBP reflect their distinct roles in RNAi. *J. Mol. Biol. 384*, 967−979.

(34) Ryter, J. M., and Schultz, S. C. (1998) Molecular basis of double-stranded RNA-protein interactions: structure of a dsRNA-binding domain complexed with dsRNA. *EMBO J. 17*, 7505−7513.

(35) Gan, J., Shaw, G., Tropea, J. E., Waugh, D. S., Court, D. L., and Ji, X. (2008) A stepwise model for double-stranded RNA processing by ribonuclease III. *Mol. Microbiol. 67*, 143−154.

(36) Stefl, R., Oberstrass, F. C., Hood, J. L., Jourdan, M., Zimmermann, M., Skrisovska, L., Maris, C., Peng, L., Hofr, C., Emeson, R. B., and Allain, F. H.-T. (2010) The solution structure of

the ADAR2 dsRBM-RNA complex reveals a sequence-specific readout of the minor groove. *Cell 143*, 225−237.

(37) Huang, Y., Ji, L., Huang, Q., Vassylyev, D. G., Chen, X., and Ma, J.-B. (2009) Structural insights into mechanisms of the small RNA methyltransferase HEN1. *Nature 461*, 823−827.

(38) Lavery, R., Zakrzewska, K., Beveridge, D., Bishop, T. C., Case, D. A., Cheatham, T., Dixit, S., Jayaram, B., Lankas, F., Laughton, C., Maddocks, J. H., Michon, A., Osman, R., Orozco, M., Perez, A., Singh, T., Spackova, N., and Sponer, J. (2010) A systematic molecular dynamics study of nearest-neighbor effects on base pair and base pair step conformations and fluctuations in B-DNA. *Nucleic Acids Res. 38*, 299−313.

(39) Cheatham, T. E., and Kollman, P. A. (1997) Molecular dynamics simulations highlight the structural differences among DNA:DNA, RNA:RNA, and DNA:RNA hybrid duplexes. *J. Am. Chem. Soc. 119*, 4805−4825.

(40) Noy, A., Pérez, A., Màquez, M., Luque, F. J., and Orozco, M. (2005) Structure, recognition properties, and flexibility of the DNA·RNA hybrid. *J. Am. Chem. Soc. 127*, 4910−4920.

(41) Dans, P. D., Pérez, A., Faustino, I., Lavery, R., and Orozco, M. (2012) Exploring polymorphisms in B-DNA helical conformations. *Nucleic Acids Res. 40*, 10668−10678.

(42) Yamashita, S., Nagata, T., Kawazoe, M., Takemoto, C., Kigawa, T., Gntert, P., Kobayashi, N., Terada, T., Shirouzu, M., Wakiyama, M., Muto, Y., and Yokoyama, S. (2011) Structures of the first and second double-stranded RNA-binding domains of human TAR RNA-binding protein. *Protein Sci. 20*, 118−130.

(43) Clemens, K., Wolf, V., McBryant, S., Zhang, P., Liao, X., Wright, P., and Gottesfeld, J. (1993) Molecular basis for specific recognition of both RNA and DNA by a zinc finger protein. *Science 260*, 530−533.

(44) Bycroft, M., Hubbard, T. J., Proctor, M., Freund, S. M., and Murzin, A. G. (1997) The solution structure of the S1 RNA binding domain: A member of an ancient nucleic acidbinding fold. *Cell 88*, 235−242.

(45) Barbas, A., Matos, R. G., Amblar, M., Lopez-Vinas, E., Gomez-Puertas, P., and Arraiano, C. M. (2009) Determination of key residues for catalysis and RNA cleavage specificity: One mutation turns RNase II into a "super-enzyme. *J. Biol. Chem. 284*, 20486−20498.

(46) Jung, S.-R., Kim, E., Hwang, W., Shin, S., Song, J.-J., and Hohng, S. (2013) Dynamic anchoring of the 3′-end of the guide strand controls the target dissociation of Argonaute-guide complex. *J. Am. Chem. Soc. 135*, 16865−16871.

(47) Pérez, A., Noy, A., Lankas, F., Luque, F. J., and Orozco, M. (2004) The relative flexibility of B-DNA and A-RNA duplexes: database analysis. *Nucleic Acids Res. 32*, 6144−6151.

(48) McMillan, N. A. J., Carpick, B. W., Hollis, B., Toone, W. M., Zamanian-Daryoush, M., and Williams, B. R. G. (1995) Mutational analysis of the double-stranded RNA (dsRNA) binding domain of the dsRNA-activated protein kinase, PKR. *J. Biol. Chem. 270*, 2601−2606.

(49) Eggington, J. M., Greene, T., and Bass, B. L. (2011) Predicting sites of ADAR editing in double-stranded RNA. *Nat. Commun. 2*, 319−1−9.